5G and UAVs for Mission-Critical Communications: Swift Network **Recovery for Search-and-Rescue Operations**

Alaa A. R. Alsaeedy · Edwin K. P. Chong

Received: date / Accepted: date

Abstract We introduce a new approach for Search-and-Rescue Operations (SAROs) to search for survivors after large-scale disasters, assuming the wireless communication network cells are partially operational and exploiting the recent trend of using Unmanned Aerial Vehicles (UAVs) as a part of the network. These SAROs are based on the idea that almost all survivors have their own wireless mobile devices, called User Equipments (UEs), which serve as human-based sensors on the ground. Our approach is aimed at accounting for limited UE battery power while providing critical information to first responders: 1) generate immediate crisis maps for the disaster-impacted areas, 2) provide vital information about where the majority of survivors are clustered/crowded, and 3) prioritize the impacted areas to identify regions that urgently need communication coverage.

Keywords Public safety communication · FirstNet · Crisis maps · Search-and-rescue · 5G · UAV

1 Introduction

Mission-Critical and Public Safety Communications (MCP-SCs) are intended to provide vital mobile wireless communication services for first responder entities, such as police and firefighters, enabling them to exchange information during emergency situations. In the following subsection, we discuss the main trends in MCPSCs. Following that, we describe a potential point of failure in current MCPSC systems.

Alaa A. R. Alsaeedy Electrical and Computer Engineering Colorado State University

Edwin K. P. Chong Electrical and Computer Engineering Colorado State University E-mail: edwin.chong@colostate.edu

E-mail: alaa.alsaeedy@colostate.edu

Finally, at the end of this section, we outline the organization of this paper in addressing the need arising from the foregoing discussion. Details of our approach, based on UAVs as network elements, begin in Section 4, after discussing posthazard issues in Section 2 and reviewing the relevant literature in Section 3.

1.1 Current MCPSC systems

Many conventional communication systems have been deployed to support MCPSCs. Since the 1930s, Public Safety Agencies (PSAs) have considered Land Mobile Radio (LMR)¹ systems as the primary means to support MCP-SCs for voice communication among emergency responders [41]. LMR systems are limited to voice and low-speed data communication. Other MCPSC systems, notably Terrestrial Trunked Radio (TETRA) and Project 25 (P25), are still currently in service, although they are inefficient in terms of spectral utilization, data rate, and cost [35, 47]. Thus, many PSAs have migrated from conventional LMR systems to more advanced mobile broadband systems. TETRA and Critical Communications Association (TCCA) have asserted that the commercial Long Term Evolution (LTE) and its next generation (5G) are the most promising technologies for MCPSCs [35, 37, 39]. For this reason, in 2012, the US developed a nationwide MCPSC system called First-Net, which uses the current LTE network as a basic platform; the US has spent \$7 billion and reserved the use of the 700 MHz band for FirstNet communications. A major recent milestone along these lines is that AT&T announced that it will spend \$40 billion toward developing FirstNet as a global wireless network dedicated to the US first responders,

¹ Basically, LMR systems are terrestrially-based networks of portable/mobile radios, base stations, and repeaters.

according to the First Responder Network Authority-AT&T 2018 contract [21].

Concurrently, the 3rd Generation Partnership Project (3GPP) has developed a specific set of mission-critical standards not only for LTE but also its successor 5G to support MCPSC functionalities. These 3GPP standards comprise Proximity-Service (ProSe) [5], Mission Critical Push to Talk (MCPTT) [2], Group Communication System Enabler (GCSE) [4], and network enablers for critical communications [1].

It is clear that there is a pressing need for reliable, extremely efficient and effective, and quick access networks for PSAs to handle life-critical missions. This interoperability between PSAs and existing commercial wireless networks will be extremely vital for MCPSC missions because the latter covers almost all the living population. For example, around 98% of the US population live in areas covered by LTE technology [28]—in this case, the PSAs can communicate even without TETRA/P25 Radio Frequency Coverage (RFC). Moreover, the mobile wireless communications over LTE/5G are beneficial not only to the PSAs but also to the people in need; they can use their smart phones for video streaming, making texts/calls, and even location sharing of User Equipments (UEs) wherever they are located in an area of consideration, called the Region of Interest (RoI). This allows PSAs to be better informed about the emergency status and hence prioritize their operations to save lives and manage the available resources. But MCPSC systems are susceptible to challenges that are unavoidable, which we address next.

1.2 Failure of current MCPSC systems

As we have seen above, there are numerous communication technologies dedicated to PSAs, the most prominent being the interworking between LTE/5G and FirstNet. For example, Los Angeles deployed about 231 sites as a first step toward the FirstNet project in March 2014 [47]. This is needed to keep the PSAs connected—anytime, almost anywhere, and in any emergency situation. At the same time, communication between PSAs and other persons (e.g., potential victims) is also crucial for life-saving purposes. However, LTE/5G and FirstNet technologies can be dysfunctional temporarily after a hazard—the network infrastructure can be devastated partially or completely by natural disasters (e.g., earthquake, hurricane, or tsunami) or even by attacks. In the worst case, the communication between the PSAs and disaster victims becomes impossible. Specifically, Search-and-Rescue Operations (SAROs), mostly locationbased missions dedicated to life-saving, become extremely difficult. In such cases, it is important for the PSAs to have some awareness of where the disaster victims are mostly located or clustered, so that the PSAs can conduct SAROs in

a timely and more effective manner. But how do we obtain sufficient information on disaster victim locations without the ability to communicate? This is the main focus of this work.

1.3 Paper outline

The rest of the paper is organized as follows. Section 2 details how a disaster impacts the serving network, addressing the most critical situations. In Section 3, we discuss related studies and address their unaddressed issues. Section 4 introduces our solution approach, considering the uncovered concerns. In Section 5, we define and formulate the necessary entities for our UE-based SARO system model. Section 6 develops screening and searching procedures that are conducted by the related *UA-gNBs*, searching for both surviving ref-gNBs and surviving UEs. Section 7 addresses an issue that arises from the overlap between the RFCs of the ref-gNB and its associated UA-gNB. Section 8 discusses the related mobility management between the ref-gNB and their associated *UA-gNB* in a disaster situation. In Section 9, we introduce a technique for the *UA-gNB* location setup, whereby it can move and search for survivors. Because each UA-gNB needs to discover a ref-gNB and adjust its initial location, these are time-consuming processes, discussed in Section 10. Section 11 details the generation of crisis maps. Section 12 is devoted to concluding remarks.

2 Network status aftermath

After a disaster, some of the wireless base stations may not survive (henceforth, we will use the abbreviation gNB for such base stations, as this is the abbreviation used in 5G). For example, after Hurricane Maria hit on September 21, 2017, 95.6% and 76.6% of the cellular sites were dysfunctional in Puerto Rico and the US Virgin Islands, respectively [38]. Accordingly, the serving network and its users in the RoI are adversely impacted in various ways, which we highlight as follows.

2.1 Lack of RFC

The surviving gNBs provide limited RFC only to UEs in close proximity. But not all UEs can exchange information with the surviving gNBs because the latter can serve only a limited number of UEs. Other UEs in the same area might receive a good level of Reference Signal Received Power (RSRP), but cannot access the available network. More specifically, these UEs try to associate with these gNBs by sending multi-access requests simultaneously without success, thus producing congested gNBs in that area.

2.2 Isolated gNBs

Potentially, the surviving gNBs are unable to communicate—the necessary links (called X2 or Xn in LTE and 5G, respectively [11]) between them are disconnected, leaving these gNBs isolated from each other. Furthermore, as long as the surviving gNBs are scattered across the RoI (and isolated), it is difficult for the PSAs to reach these UEs by wireless communication. In such cases, the SAROs are crucial—victims might be trapped or isolated and risk not being found and rescued.

2.3 Cell-edge UEs

At the cell edges of a surviving gNB, UEs might struggle to associate with the gNB because of low RSRP levels. Moreover, parts of the RoI might have no RFC at all. In this case, the UEs start searching for a suitable cell (gNB) to camp on, initiating what is called the Cell Search Procedure (CSP) [7,8]. Typically, as long as no suitable serving cell is found, the UEs continue to perform the CSP, attempting to find one. This gives rise to a power consumption problem for the UEs—most UEs are battery-limited, and hence conducting CSPs continually without success drains the battery power in these UEs. Eventually, they will be out of service and unreachable, remaining lost even when the RFC is restored.

In this context, this paper deals with large-scale disasters in which the RFC area is limited or nonexistent, leaving the surviving UEs struggling to get connected.

3 Related studies

Many different solutions have been introduced to address the problem of lack of wireless communication between the PSAs and victims in emergency situations. Here, we classify the existing solutions for network restoration into three main groups based on the particular approaches taken, as follows.

3.1 Deploying wireless equipment into RoI

Early solutions have been proposed for emergency managements and triaging patients, allowing first aid teams to prioritize their efforts, named "ARTEMIS" and "CodeBlue," as in [33] and [31], respectively. These two systems are similar in design but differ in data transmission protocols. The two systems deploy wireless-based sensors (for monitoring victims' vital signs) into the RoI. For the data transmission, in [33], medics (with hand-held devices) can move within a

deployed ad-hoc wireless network, in which data from multiple devices can be transmitted to remote high-level medical personnel. In [31], the authors propose to create a dedicated wireless sensor network throughout the RoI, comprising multi-purpose sensors (e.g., location and biomedical sensors), used for data transmission.

For military and battlefield assistance, the author of [46] develops a system to track and identify causalities in severe environments, called the Tactical Medical Coordination System (TacMedCS). This system comprises a set of hand-held devices to collect vital signs of victims (including their locations and IDs), providing near real-time awareness of casualty status and allowing medics to respond quickly. In the absence of wireless communication, TacMedCS uses satellite phones for data transmission.

Recently, unlike the solutions in [31, 33, 46], Nokia introduced man-portable and vehicle-mounted LTE eNBs to provide temporary LTE RFC for the RoI [45], recovering the network and enabling the PSAs to communicate with disaster victims.

The solutions in [31,33,45,46] are effective in dealing with small-scale emergency situations, where the PSAs or vehicle-mounted eNBs can move freely into the RoI. However, in large-scale disasters (e.g., earthquakes), such solutions can fail because of the difficulty in moving into the disaster area quickly (e.g., because of ground rupture and landslides).

3.2 Network recovery using D2D communication

A well-known technique has emerged to enhance the overall performance of current LTE networks, called Device-to-Device (D2D) communication (also called the 3GPP ProSe feature in LTE) [20]. This is to enable UEs in close proximity to communicate through direct links without passing through eNBs. Exploiting this feature, the authors of [24] introduce a D2D communication scheme and a clustering procedure for network recovery. This study addresses the energy efficiency and battery lifetime of UEs, but it requires special devices to be deployed that have high transmission power, long battery lifetime, and the ability to control radio resources. These are critical requirements because such devices are not widely used or available to the end-users. Furthermore, the PSAs cannot easily deploy such devices in large-scale disasters (as detailed in Section 3.1).

Similarly, the authors of [15] propose an efficient network architecture using D2D communication for disaster situations when the network infrastructure is partially unavailable. The authors of [15] use multi-hop concepts of D2D to extend the network coverage of functional eNBs to regions where the coverage is unavailable. This is done by using Relay Nodes (RNs) that route wireless coverage to-

ward uncovered areas. Although this work shows some benefits of using multi-hop D2D for extending network coverage and reducing transmission power, its availability would be limited—the RNs are mostly typical UEs, which are limited in battery power and processing capabilities. Moreover, if these RNs move, the system would select new suitable RNs; this process impacts the system complexity and stability (because of frequent association and dissociation).

To address the power constraint in the solution of [15], the authors of [16] introduce a Wireless Energy Harvesting (WEH) scheme, exploiting the ability to convert the received RF into energy. In this scheme, the RNs are able to transmit data and energy to UEs via RF. Although this work has shown that WEH can reduce the power consumption of UEs, UEs need to be equipped with RF energy-harvesting circuitry, which is not available in common UEs. Also, when RNs move, it would impact the system stability.

Like in [16], the authors of [29] introduce an energy-efficient UE discovery scheme under interference constraints, called D2D Discovery Maximization (D2D-DM), providing a switching capability for discovery modes (half-duplex and in-band full-duplex). Specifically, when the signal-to-interference-noise ratio of a D2D link drops below a specified threshold, the discovery mode switches from half-duplex to in-band full-duplex. In addition, for battery-limited UEs, the authors adopt an open-loop power control scheme to reduce power consumption. According to [29], the D2D-DM scheme shows a significant improvement in the number of discovered UEs as compared to static resource allocation and the random backoff scheme.

Recently, in the context of WEH, the authors of [32] propose a D2D-based framework with energy-efficient clustering and routing for disaster communication relief. This solution shows a significant improvement in terms of power consumption and end-to-end transmission delay compared to the solutions in [15,16]. The authors use a Particle Swarm Optimization (PSO) algorithm for routing and clustering. PSO is a time consuming algorithm, especially when the search space is large and it does not guarantee finding an optimal solution [43]. The use of PSO adds to the overhead and complexity, which compromises the success in dealing with large-scale disasters. Solutions that add no overhead are naturally preferable.

3.3 Network recovery using UAV communication

Recently, some studies have proposed the use of Unmanned Aerial Vehicles (UAVs) as mobile gNBs for rapid network recovery. These UAVs are useful in a variety of applications, especially in wireless mobile communication [30]. More recently, this attention has brought current LTE closer to supporting UAV communication [36]. The authors of [42] provide a comprehensive survey of using UAVs in public

safety communication, highlighting power consumption issues. In addition, the authors propose a multi-layered architecture for emergency situations, providing alternative paths for emergency communications. The study in [42] highlights a variety of issues that are related to UAV placement, UAV communication links, and UAV trajectory plans.

Exploiting this trend, the authors of [34] propose an optimization scheme to place the UAVs, improving the 5th percentile capacity of LTE networks. This UAV placement scheme aims to improve the network throughput. However, in [34], the UAV locations are optimized using brute-force search, which can be prohibitively time consuming. Moreover, the placement scheme of [34] depends on how the surviving gNBs are distributed. Doing so does not account for where the deployed UAVs are mostly needed; it ignores where the majority of UEs are located.

To provide full coverage to all users in the RoI, the authors of [23] propose a solution scheme in which a very large number of UAVs are deployed to cover all UEs. Although the scheme provides full RFC, it is inefficient and possibly impractical; the complexity is proportional to the size of the RoI, and the scheme might provide unnecessary RFC.

In sum, the preceding studies have proposed many solution schemes for wireless network restoration after hazards. However, they do not focus on where the majority of UEs are located to provide the necessary coverage in a timely manner. Furthermore, at the time of writing this paper, no solution provides the corresponding PSAs with information on surviving UE locations for the purpose of SAROs. In this paper, we address these issues.

4 Solution approach

4.1 Issues to be considered

The issues highlighted in Section 2 are the main focus of this paper. As we have seen from the recent studies, the focus has been on how to provide RFC in the RoI instead of finding the UEs. Specifically, it is crucial not only to provide RFC but also to locate these UEs—where and how the UEs are clustered. After disasters, the location distribution of surviving UEs is likely to be nonuniform. Estimating this distribution provides critical situational awareness to PSAs and helps to focus the use of scarce resources. In addition, it is important to locate these UEs without their assistance—these UEs might be unable to telecommunicate because of the lack of wireless service, network congestion, injuries, unconsciousness, or even unresponsiveness. Awareness of victim locations is a very critical requirement for the MCPSCs, often racing against time.

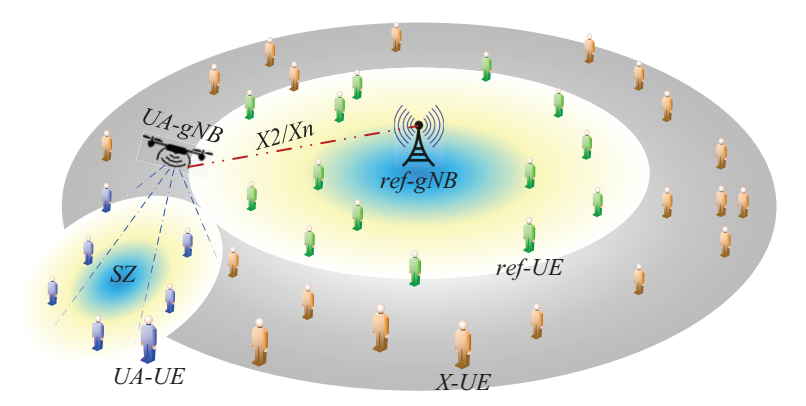


Fig. 1 Illustrative example showing the SARO entities

4.2 Proposed approach

Considering the above issues, we propose a new method for SAROs to find potential survivors by finding their UEs without their assistance, even in the absence of RFC, while providing temporary RFC based on certain prespecified priorities (e.g., number of survivors in each sub-area of the RoI; later, we call this sub-area the *Searching Zone (SZ)*). Conducting SAROs by searching for surviving UEs to locate individuals is effective especially because these UEs have become more ubiquitous—each individual (likely) is equipped with at least one of the following: smart phones, tablets, smart watches, or even embedded sensors in the human body or clothing; most of these devices are embedded with RF equipment. This is a quick way to provide vital information to the PSAs even before they arrive at the scene.

In this paper, the SAROs are based on the idea that each individual has its own UE and potentially is still alive and willing to be found, and hence we call our solution *UE-based SAROs*. Specifically, this work is mainly intended to (among other functions, as we will see later) generate immediate crisis maps², providing information to the corresponding PSAs to prioritize their operations in disaster-affected regions. Essential entities of *UE-based SAROs* are discussed next.

5 UE-based SARO system model

In our solution, we use UAVs as mobile gNBs, called *UA-gNBs*, as a part of the network infrastructure in the RoI. We assume that the impacted network is only *partially* dysfunctional; some of gNBs are still able to broadcast and exchange signaling. Before proceeding further, we define the essential entities in our solution (illustrated in Fig. 1 in color for clarity), as below.

5.1 Entity definitions

- 1. ref-gNBs: These are the surviving gNBs, called reference gNBs (ref-gNBs); see Fig. 1. These ref-gNBs provide Radio Resources Management (RRM) functionalities, such as resource allocation, scheduling, and mobility control [6, 13]. The deployment of a UA-gNB does not need its own RRM. Instead, the ref-gNBs provide the necessary RRM to the corresponding UA-gNBs. This is to minimize the load on these UA-gNBs, to address limitations in battery power and processing capabilities.
- 2. UA-gNBs: These are the deployed UAVs, as mentioned above. We use them to provide mobile picocells with range expansion capabilities, with a cell radius of 100-300 m and transmit power of 24–33 dBm [26]. Each UAgNB has five main functions: 1) search for a ref-gNB to associate with, establishing X2/Xn interfaces³; 2) search for surviving UEs that are actively seeking a serving cell to camp on, around the detected ref-gNB (based on a screening procedure we define later), broadcasting UE-specific control messages; 3) feed back the screening results to the corresponding ref-gNB, via X2/Xn, for further processing/analysis; 4) provide the necessary RFC according to where the UEs are in need (decisions made by the ref-gNB); 5) while conducting the screening procedure, the UA-gNBs and ref-gNBs broadcast paging messages to the corresponding UEs, including emergency alert messages, using the already existing public warning system in LTE, known as Commercial Mobile Alert System [10]. For example, the UA-gNBs may broadcast the following message: "If your location is safe, stay; otherwise go the nearest safe location and remain there. Refrain from using your mobile phone to conserve battery; we will reach you by phone."

² Google Crisis Map [27] is a well-known example of a crisis map, but its availability needs Internet connectivity and does not provide immediate information about how and where individuals are distributed.

³ Essential interfaces between gNBs in LTE/5G networks for exchanging necessary control signaling [11].

- 3. *ref-UEs*: These are surviving UEs that have been associated and registered with *ref-gNBs* (e.g., because of their close proximity) as shown in Fig. 1 (in green).
- 4. *UA-UEs*: These are surviving UEs that have been discovered and associated with *UA-gNBs* after the screening procedure. As mentioned above, the association information will be sent to the corresponding *ref-gNB* for further processing. The *UA-UEs* are shown in Fig. 1 (in blue).
- 5. *X-UEs*: These are surviving UEs but not associated to any gNB. While the RFC is not available (or the received RSRP is too low), the *X-UEs* continually execute the CSP, which consumes the battery power of the UEs. These *X-UEs* need to be found as quickly as possible; otherwise, as stated before, they might go out of service. Fig. 1 shows these *X-UEs* (in brown).
- 6. Searching Zones (SZs): To facilitate the screening and searching for X-UEs, the area around each ref-gNB is partitioned into a set of sub-areas, called SZs. Each UA-gNB performs the screening procedure in its own assigned set of SZs. These SZs are known to the ref-gNBs, as detailed later in Section 9. The SZs are also used to generate crisis maps called UEBCMs (defined below).
- 7. Priority-Driven RFC (PDRFC): After the screening procedure, decisions will be made by each ref-gNB to identify the areas that are in need of immediate RFC based on UE clustering, which we call PDRFC. The resulting PDRFC includes a set of SZs arranged in priority orders.
- 8. *UE-Based Crisis Map (UEBCM)*: Based on the collected information (e.g., *PDRFC*), each *ref-gNB* generates its own crisis maps, called *UEBCMs*. These maps will contain all the necessary information (*ref-gNB* locations, surviving UE locations, and the corresponding RSRP measurement reports). These maps will be accessible to the PSAs later.

5.2 Entity notation

For ease of presentation, we introduce some precise notation for the entities defined in the last section:

- 1. ref-gNBs: We denote the set of their locations by $\mathcal{R} = \{(x_i^{ref}, y_i^{ref}) : i = 1, 2, \dots, R\}$, where (x_i^{ref}, y_i^{ref}) is the location of $ref-gNB_i$ and R is the total number of the detected ref-gNBs. These form a sub-set of all gNBs, whose locations are denoted by the set \mathcal{A} (i.e., $\mathcal{R} \subset \mathcal{A}$).
- 2. UA-gNBs: We denote the set of associated UA-gNB locations relevant to ref- gNB_i by $\mathcal{L}_i = \{L_{i,j} : j = 0, 1, \dots, J_i 1\}$, where j is the index of the underlying SZ and J_i is the total number of the SZs around ref- gNB_i (defined in item 5 below), as detailed in Fig. 2 ($L_{i,j}$ and J_i are calculated in Section 9). Here, we assume that for

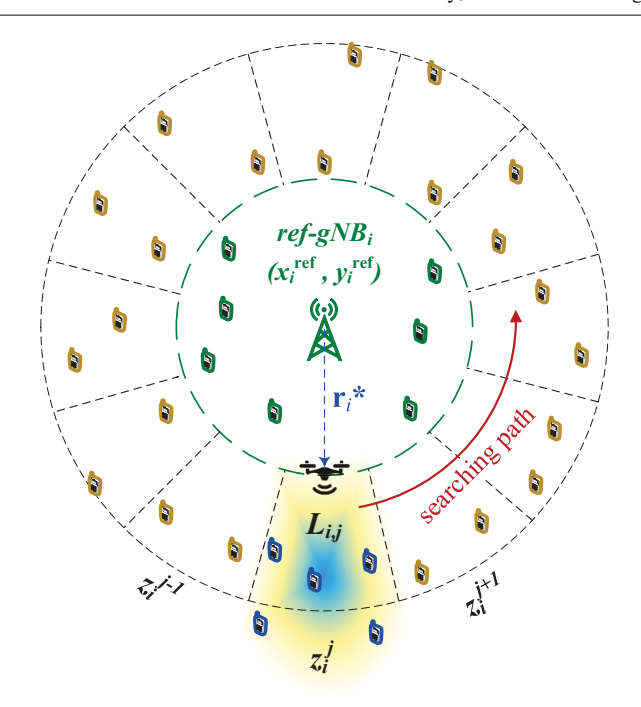


Fig. 2 UA-gNB searching model

- each detected ref- gNB_i there is one associated UA- gNB_i (they have the same index i, as defined in item 1 above).
- 3. ref-UEs: We denote the set of ref-UEs associated with ref- gNB_i by $G_i = \{ue_{i,q}^{ref}: q = 1, 2, ..., Q_i\}$, where Q_i is the total number of associated UEs. For example, if ref- gNB_3 has a total of 100 associated UEs, then $G_3 = \{ue_{3,1}^{ref}, ue_{3,2}^{ref}, ..., ue_{3,100}^{ref}\}$.
- 4. UA-UEs: We denote the set of UA-UEs associated with $UA-gNB_i$ within SZ j by $S_i^j = \{ue_{i,p}^j : p = 1, 2, ..., P_i^j\}$, where P_i^j is the total number of associated UEs within zone index j. For example, suppose that $UA-gNB_5$ has screened the zone with index 2 (located at $L_{5,2}$) and detected 20 UEs. Then, the set of these UEs is identified as $S_5^2 = \{ue_{5,1}^2, ue_{5,2}^2, ..., ue_{5,20}^2\}$.
- 5. *SZs*: We denote the *SZs* surrounding ref- gNB_i by $Z_i = \{z_i^j : j = 0, 1, ..., J_i 1\}$, where J_i is defined in item 2 above. For example, if ref- gNB_2 has 12 surrounding SZs, then $Z_2 = \{z_2^0, z_2^1, ..., z_1^{21}\}$. The set Z_i surrounds the cell edge of the corresponding ref- gNB_i .

6 UA-gNB searching procedures

The *UA-gNB* performs two essential searching procedures. The first (detailed in Section 6.1) is to find a *ref-gNB* to obtain the required RRM. Second (detailed in Section 6.2), and after association with a *ref-gNB*, the *UA-gNB* starts searching for surviving UEs (*X-UEs*), which likely are starving for a serving cell. Because the *UA-gNBs* and UEs are battery-power limited, the following concerns arise: 1) the *UA-gNB*

should find a *ref-gNB* as quickly as possible to save its battery capacity; 2) the *X-UEs* (in brown in Fig. 1) should be found and located within a reasonable time, by the searching *UA-gNB*, before many of these UEs run out of battery power. These concerns involve time-critical requirements. Thus, the search schemes must be time efficient, as described next.

6.1 Procedure for finding ref-gNB

To locate a *ref-gNB*, the *UA-gNB* can scan the whole RoI or use some prediction algorithms, but under the above requirements, such searching schemes are too inefficient. Our procedure involves two essential schemes, by which the searching *UA-gNB* finds its best candidate location and optimal distance from the corresponding *ref-gNB*, as we will describe in Sections 6.1.1 and 6.1.2, respectively.

To expedite the searching efforts and develop time-efficient strategies, we consider the following factor. Typically, all the gNBs at locations in set \mathcal{A} are already deployed according to a predefined plan—the locations in \mathcal{A} are distributed based on where the RFC is most needed (e.g., hot spots and crowded areas). Hence, the locations in \mathcal{A} (also defined by their Physical Cell Identifications (PCIs)) are known to the UA-gNBs. But initially (after hazards), the UA-gNBs do not know \mathcal{R} ; i.e., where the potential ref-gNBs are located. In other words, the UA-gNBs need to find and locate operational potential ref-gNBs—this is necessary for association purposes (for RRM; see Section 5.1). By exploiting the known \mathcal{A} , we introduce the following scheme for UA-gNBs to find ref-gNBs to associate with.

6.1.1 Cluster Centroid-based Search (CCBS)

In this scheme, the UA-gNBs localize all the ref-gNBs (\mathcal{R}) simultaneously with low computation overhead, which we detail in the following steps:

- The RoI is partitioned, based on the location set \$\mathcal{H}\$, into \$K\$ groups using some well-known partitioning algorithm, such as \$k\$-means++ [19]\$. This is a simple and fast way to find points that serve as centroids for each partition subset of \$\mathcal{H}\$, to serve as initial searching points for \$UA\$-gNBs\$. These initial points are defined by the set \$\mathcal{K} = \{(x_k^{ua}, y_k^{ua}) : k = 1, 2, 3, ..., K\}\$, where \$K\$ is the total number of cluster centroids. If we assume that for each defined cluster \$k\$ there is exactly one searching \$UA\$-gNB\$, \$K\$ will be equal to the total number of the searching \$UA\$-gNBs\$, and hence (based on the previous assumption in Section 5.2, item 2), there will be one \$ref\$-gNB\$ for each cluster \$k\$, as illustrated in Fig. 3.
- 2. In the *CCBS* scheme, for each cluster centroid, there is one *UA-gNB* located initially at (x_k^{ua}, y_k^{ua}) ; *K UA-gNBs* are assigned, one each, to all *K* cluster centroids in \mathcal{K} .

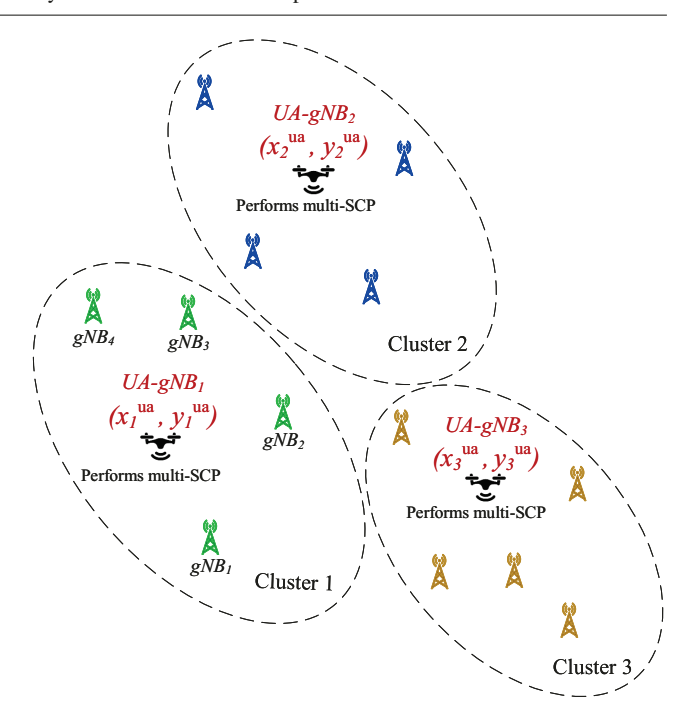


Fig. 3 Illustrative example showing *UA-gNBs* centers at cluster centroids, using k-means

Because *UA-gNBs* are deployed at some altitude, it is likely for them to receive Line-of-Sight (LoS) signaling from multiple potential *ref-gNBs*. Furthermore, deployment of *UA-gNBs* at appropriate altitudes ensures that the ground UEs would receive good levels of RSRP while getting screened by these *UA-gNBs*, as we will see in Section 6.2. The LoS distance is denoted by **r**, as illustrated in Fig. 4.

3. While flying around its initial location (from the set \mathcal{K}), the UA-gNB performs multi-cell search (using the conventional SCP). Once the UA-gNB detects a serving cell, the PCI of the decoded cell is identified (a ref-gNB found), and hence its location, (x_i^{ref} , y_i^{ref}), becomes known. In this case, the UA-gNB associates with this ref-gNB for exchanging the necessary information, detailed further in Section 10.1.

6.1.2 UA-gNB optimal distance

The associated UA- gNB_i has to search for X-UEs, which are mostly located at the cell edge of ref- gNB_i (detailed in Section 2.3 and shown in Figs. 1 and 2), assuming the ref-UEs, those in G_i , have already associated with ref- gNB_i . We describe the procedure to search for X-UEs in the following steps:

1. UA- gNB_i sets its initial distance (\mathbf{r}_i) from ref- gNB_i such that it can search its SZs, \mathcal{Z}_i , circulating around the cell

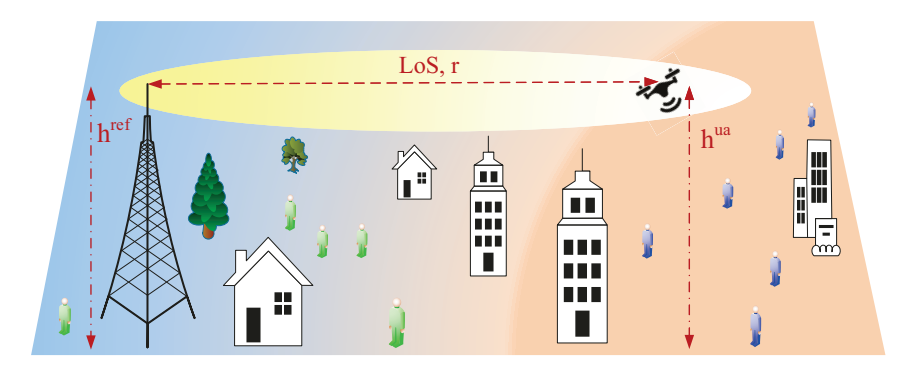


Fig. 4 Illustrative example showing the LoS and height conditions

edge. The initial distance is calculated as follows:

$$\mathbf{r}_{i} = \sqrt{(x_{i}^{\text{ref}} - x_{k}^{\text{ua}})^{2} + (y_{i}^{\text{ref}} - y_{k}^{\text{ua}})^{2}},$$
(1)

where $(x_i^{\text{ref}}, y_i^{\text{ref}})$ and $(x_k^{\text{ua}}, y_k^{\text{ua}})$ are defined in \mathcal{R} and \mathcal{K} , respectively. To locate the ref- gNB_i cell edge, we use the Path Loss (**PL**) to calculate a maximum distance, called \mathbf{r}_i^* , subject to the constraint that **PL** does not exceed a predefined value $\mathbf{PL}_{\text{threshold}}$. This constraint is required to maintain the communication link between them (Xn). In this context, we consider the following **PL** formula, which is widely used in the literature (for urban and suburban areas) for system-level simulations [12]:

$$\mathbf{PL}(\mathbf{r}_{i}) = 40 \cdot (1 - 4 \cdot 10^{-3} \cdot \mathbf{h}_{i}^{\text{ref}}) \cdot \log_{10}(\mathbf{r}_{i}) - 18 \cdot \log_{10}(\mathbf{h}_{i}^{\text{ref}}) + 21 \cdot \log_{10}(f) + 80 \ dB,$$
 (2)

where \mathbf{r}_i is the distance (in kilometers) between the *ref-gNB_i* and *UA-gNB_i*, f is the carrier frequency in MHz, and $\mathbf{h}_i^{\text{ref}}$ is the *ref-gNB_i* antenna height (in meters), measured from the average rooftop level.

2. Now we calculate the maximum distance \mathbf{r}_i^* (the radius of the *ref-gNB_i* cell edge), which is the solution to the following optimization problem:

$$\mathbf{r}_{i}^{*} = \arg\max_{\mathbf{r}_{i}} \mathbf{PL}(\mathbf{r}_{i})$$

$$\mathbf{r}_{i}$$

$$\mathbf{r}_{i} \in \mathbf{PL}(\mathbf{r}_{i}) \leq \mathbf{PL}(\mathbf{r}_{i})$$
(3)

subject to $PL(\mathbf{r}_i) \leq PL_{\text{threshold}}$.

After solving (3), UA- gNB_i will be placed at distance \mathbf{r}_i^* from its ref- gNB_i , screening around the cell edge, as shown in Fig. 5. This will help the uncovered X-UEs to associate with UA- gNB_i while screening its SZs. But this placement gives rise to an issue involving overlapping RFCs, which we highlight in Section 7.

6.2 Procedure for finding X-UEs

After finding the optimal placement \mathbf{r}_{i}^{*} , the associated *UA-gNB_i* is ready to surveil the corresponding *ref-gNB_i* cell

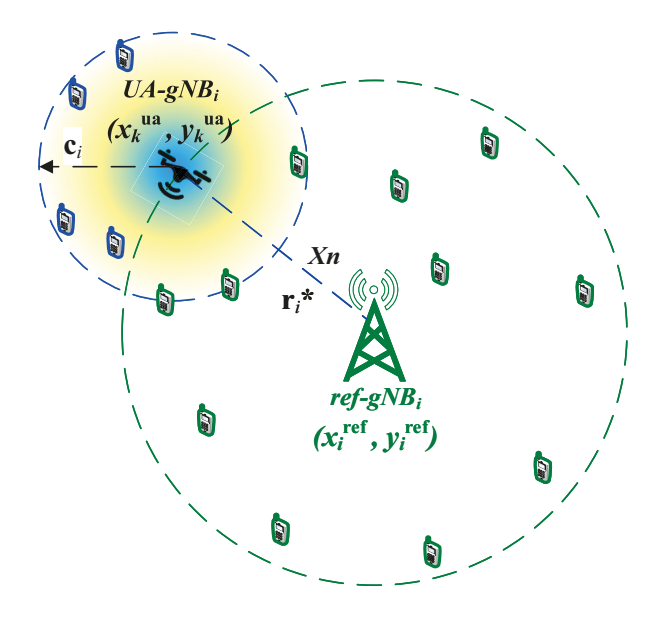


Fig. 5 Maximum distance according to (3)

edge, as described in Section 5.1. Specifically, UA- gNB_i follows a path around the cell border at a distance of \mathbf{r}_i^* from ref- gNB_i . Here and for ease of presentation, we assume that the cell edge is a circular boundary; the searching model is detailed in Fig. 2. As defined in Section 5.2, item 5, there are SZs around ref- gNB_i , called z_i^j (introduced in Section 9), in which UA- gNB_i searches for X-UEs. Specifically, ref- gNB_i assigns its SZs, z_i^j , to the associated UA- gNB_i . The following steps elaborate on the screening procedure:

- In each z_i^J, when X-UEs are exposed to the RFC of UA-gNB_i (at location L_{i,j}), they normally initiate the CSP.
 As a result, UA-gNB_i becomes the serving cell for all the detected UEs in the underlaying zone j.
- 2. All *X-UEs* in z_i^j that are found (by $UA-gNB_i$) will be registered as UA-UEs (to differentiate them from those that are already associated with the corresponding $ref-gNB_i$). As stated in Section 5.2, item 4, the number of these UA-UEs is defined by S_i^j —that is, for each z_i^j , there is a corresponding S_i^j .

3. The context information⁴ of the UA-UEs in S_i^j will be stored in $UA-gNB_i$. To detect as many X-UEs as possible, $UA-gNB_i$ may circulate around the cell edge multiple times. In this case, every time $UA-gNB_i$ makes a new round, it does not need to re-register the already detected UA-UEs. Moreover, after association, $UA-gNB_i$ broadcasts control messages to the corresponding UA-UEs to change their RRM status to the INACTIVE state (as described in [18], Section 6.1). This will save more power in the battery-limited UEs and provide very fast network access with lightweight signaling overhead when UA-UEs (in the INACTIVE state) are exposed multiple times to the RFC of $UA-gNB_i$.

In this context, we will discuss a mobility management issue in our *UE-based SAROs* to meet its critical requirements (signaling overhead and battery power consumption) in Section 8.

7 UA-gNB overlapping RFC issue

As discussed in Section 6.2, the associated $UA-gNB_i$ searches for X-UEs, mostly located close to the cell edge of the corresponding ref- gNB_i . This UA- gNB_i does so at the optimal distance \mathbf{r}_i^* (calculated in (3)) from its ref- gNB_i . But this placement gives rise to the following issue.

As we see in Fig. 5, the RFCs of $UA-gNB_i$ and $ref-gNB_i$ are overlapping. In this case, some of the UEs in G_i (more precisely, those in the intersected area, $\mathcal{G}_i \cap \mathcal{S}_i^J$, of the current SZ) would initiate cell (re)selection⁵ procedures each time they are exposed to the RFC of UA- gNB_i . This might occur when these UEs receive higher levels of RSRP from UA- gNB_i than from ref- gNB_i . More specifically, these UEs (those in $G_i \cap S_i^J$) may switch back and forth between these two cells (UA- gNB_i and ref- gNB_i), resulting in what is often called the toggling effect. This increases the signaling load on the both serving cells and their associated UEs. Moreover, initiating multi-cell (re)selection drains battery power in these UEs. Furthermore, as we will see later, this will impact the accuracy of the generated *UEBCM*. Specifically, each z_i^I has its own associated UEs and this is required because UE locations are defined by their serving cell (whether UA- gNB_i or ref- gNB_i). In addition, all UEs within the overlapped RFC will receive relatively high intercell interference.

It would appear that this problem can be solved easily by increasing \mathbf{r}_i^* such that the RFC of UA- gNB_i lies outside the RFC of ref- gNB_i (to achieve no overlap, \mathbf{r}_i^* must be increased by \mathbf{c}_i). But by doing so, the necessary connection (Xn) will be lost, and hence this is not a feasible solution. To deal

with this issue, we introduce two different techniques (which can be used separately or together), involving no additional computation cost. In both techniques, we need to keep the distance \mathbf{r}_i^* unchanged, but ensure that the RFCs of UA- gNB_i and ref- gNB_i are nonoverlapping.

7.1 Beamsteering antenna

Beamsteering antennas are widely used in LTE and are expected to be used in upcoming 5G networks [14,40]. In this technique, the antenna radiation pattern can be electrically steered to a desire direction without physically moving the antenna [44]. In our case, the antenna radiation pattern of the UA- gNB_i should be steered in such a way that its RFC lies outside the RFC of ref- gNB_i , as we illustrate in Fig. 6. Specifically, the center of the coverage area (labeled \mathbf{o} in Fig. 6) is shifted to the left by distance \mathbf{c}_i . Accordingly, the main beam (as shown in the top illustration in Fig. 6) is shifted by angle \mathbf{a}_i , as shown in the bottom illustration in Fig. 6. For that purpose, the angle \mathbf{a}_i is calculated from the following formula: $\mathbf{a}_i = \tan^{-1} \mathbf{c}_i/\mathbf{h}_i^{\mathrm{ua}}$, where \mathbf{c}_i is the radius of the cell coverage and $\mathbf{h}_i^{\mathrm{ua}}$ is the height for the corresponding UA- gNB_i .

By using this technique, the overlapping issue is addressed (to avoid multi-cell (re)selections). Moreover, because the center of the *UA-gNB* coverage area is shifted away from the *ref-gNB* cell edge, it will cover more *X-UEs* beyond the cell edge.

7.2 Access control

In this technique, unlike the above one, the overlapping is allowed (as in the top illustration in Fig. 6). But the multicell (re)selection (i.e., toggling effect) in the overlapping area is avoided using what is called the "barred cell" access control [9]. Under extreme circumstances (e.g., emergency situations), there is likely to be a huge number of UE access attempts triggered simultaneously—this leads to service degradation and lack of radio resources. To deal with this issue, when it is appropriate, network operators apply the "barred cell" mechanism to prevent many UEs from initiating simultaneous access attempts toward a certain set of gNBs, preventing the network from being overloaded. In this case, the gNBs broadcast cell access restrictions via system information messages to their associated UEs. In doing so, the corresponding UEs are prohibited from triggering multiaccess attempts.

Taking advantage of this mechanism, the UEs in the overlapping area $(\mathcal{G}_i \cap \mathcal{S}_i^j)$ would no longer switch back and forth between the two RFCs. In other words, the UEs in \mathcal{G}_i are not allowed to make access attempts toward UA- gNB_i .

⁴ Includes UE-specific configuration parameters [3].

⁵ Assuming these UEs are in idle mode; otherwise, they would undergo handover.

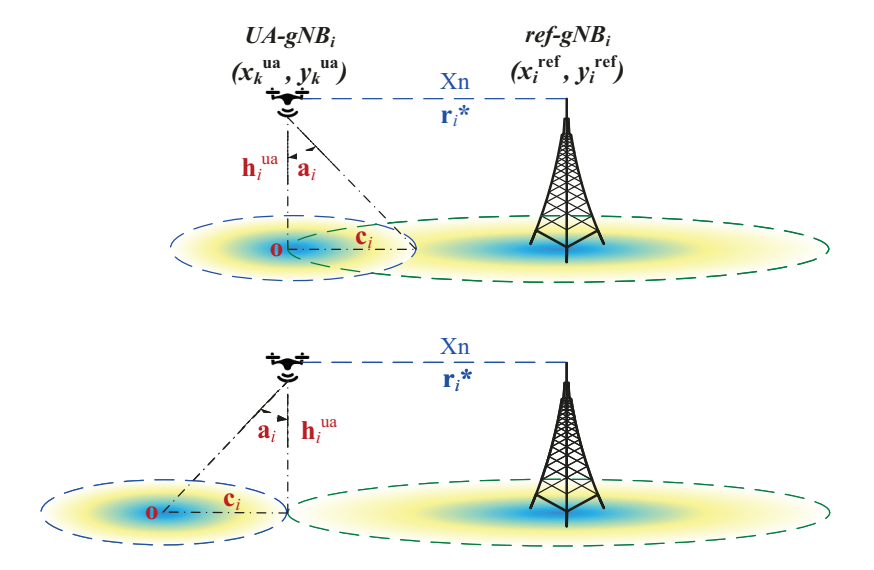


Fig. 6 Avoiding RFC overlap using beamsteering

Likewise, the UEs in S_i^j are prohibited from accessing *ref-gNB_i*.

Note that the two techniques above prevent the toggling effect, and hence will save more power in the battery-limited UEs and provide lightweight signaling overhead. But the beamsteering method provides a larger RFC area than the "barred cell" access control method, as shown in Fig. 6—this is because the former shifts the center of its RFC away from the cell edge while the latter still results in overlapping RFC.

8 Mobility management for UE-based SAROs

In 5G networks, each gNB manages and controls its own associated UEs, including providing Mobility Management (MM) (see [18], Section 5.1). This MM imposes signaling overhead that is unsuitable for *UA-gNBs* because the latter are limited in battery power and processing capabilities. Instead, MM tasks, including RRM, will be handled by the corresponding *ref-gNB*, which is much more powerful than the *UA-gNB*.

Typically, in 5G, two essential MM procedures are involved to track and locate mobile UEs within the network, called *Tracking Area Update (TAU)* and *Paging* [18], which burden not only the serving network but also the associated battery-limited UEs. In this context, we propose in [17] efficient MM schemes that can be applied to mission-critical applications—that is, it can meet the critical requirements imposed by *UE-based SAROs*. We call this MM solution *gNB-based UE Mobility Tracking (gNB-based UeMT)*, in which *TAU* is avoided and *Paging* delay is improved, enhancing the overall network performance, including power consumption in UEs and lightweight signaling overhead.

Table 1 Equivalence of *gNB-based UeMT* and *UE-based SAROs* entities

gNB-based UeMT	UE-based SAROs
anchor-gNB	ref-gNB
Home-UE	ref-UE
Visiting-UE	UA-UE
Visiting-gNB	UA-gNB

As we have seen in *UE-based SAROs*, two types of UEs are defined: *ref-UEs* and *UA-UEs* based on their associated gNBs (*ref-gNB* and *UA-gNB*, respectively). These two base stations interact together to handle UE mobility. As we have described in our *gNB-based UeMT* solution, a gNB takes over the responsibility of the MM—this gNB is called *anchor-gNB* (or *Home-gNB*), as defined in [17], Section IV-A. To apply *gNB-based UeMT* for *UE-based SAROs*, we now define the equivalent entities for both systems, as in Table 1.

It is worth mentioning here that our MM solution, gNB-based UeMT, by design has the potential to deal with mission-critical applications. This can be achieved by choosing the relevant control system parameters appropriately (refer to Section IV-B in [17]). For example, to guarantee that the inter-Paging delay between the refgNB and its associated UA-gNB does not exceed a predefined value, the relevant system parameter, called Calculated inter-Paging Delay (CiPD) index should take a value index equal to CiPD_0—this is to maintain the CiPD at below 1 msec. Applying gNB-based UeMT and according to its features, the ref-gNB will take over the responsibility of MM tasks (to reduce the load on the UEs and UA-gNBs), offer lightweight signaling overhead (it achieves about 92% reduction in the relevant load [17]), and provide always-

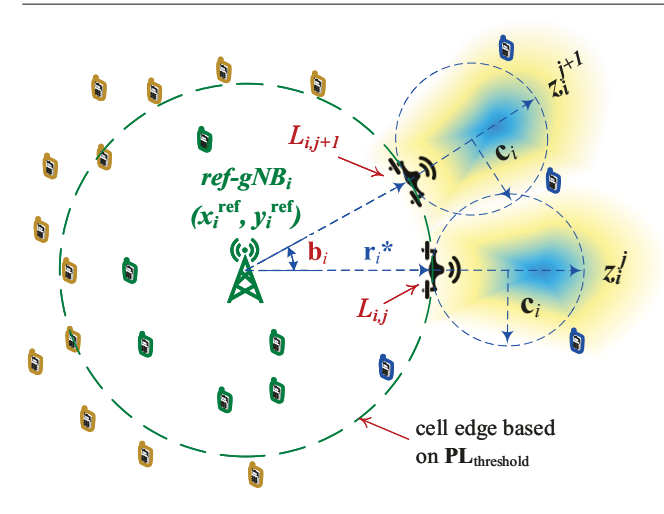


Fig. 7 *UA-gNB*_i screening locations

known UE locations—these are important for *UE-based SAROs*.

9 *UA-gNB* location setup for *SZs*

As we have stated earlier (see Fig. 2), after calculating \mathbf{r}_i^* , UA- gNB_i starts screening around the corresponding cell edge. But so far, it is not clear that how UA- gNB_i moves around the cell edge within the radius \mathbf{r}_i^* . Recall the set $\mathcal{L}_i = \{L_{i,j} : j = 0, 1, \dots, J_i - 1\}$. As mentioned before, $L_{i,j}$ represents the UA- gNB_i location relevant to its ref- gNB_i cell edge while in SZ j. In other words, each value of j corresponds to a specific location of UA- gNB_i on the cell edge path. So, we need to find these locations for each value of j, where UA- gNB_i is located. We explain how to find these coordinates for each value of j. When screening SZ j, the UA- gNB_i should be located at $L_{i,j}$, which is defined (in polar) as:

$$L_{i,j} = \mathbf{r}_i^* / j \cdot \mathbf{b}_i$$
 , $j = 0, 1, ..., J_i - 1$, (4)

where $L_{i,0} = \mathbf{r}_i^*/\underline{\mathbf{0}}$ is the initial location and J_i is the total number of the SZs around ref- gNB_i (calculated below). Now, we calculate the angle \mathbf{b}_i as follows. After completing the screening process, UA- gNB_i moves to the next SZ at $L_{i,j+1}$ such that the distance between its previous and next positions, denoted by $d(L_{i,j}, L_{i,j+1})$, is approximately equal to its RFC radius, the quantity labeled \mathbf{c}_i in Fig. 7 (the illustration in Fig. 7 assumes beamsteering, as detailed in Section 7.1). This is to keep the SZs separated and minimize the overlap between their corresponding RFC, as Fig. 7 illustrates. Note that even when a swap occurs, there is no confusion among the detected UEs (to which SZ they belong); this is because UA- gNB_i registers the detected UA-UEs such that each SZ has its own UEs, which means that $S_i^j \cap S_i^{j+1} = \emptyset$.

Table 2 Information table for each ref-gNB_i-UA-gNB_i pair

\mathcal{Z}_i	UA-gNB locations (polar)	UE densities	Average RSRP (dBm)
z_i^0	$L_{i,0}$	\mathcal{S}_i^0	RxLev#0
z_i^1	$L_{i,1}$	\mathcal{S}_i^1	RxLev#1
$Z_i^{J_i-1}$	L_{i,J_i-1}	$\mathcal{S}_i^{J_i-1}$	$RxLev#J_i - 1$

Table 3 Association table for each ref- gNB_i

$\mathcal R$	ref - gNB_i	G_i , set of ref-UEs	Average RSRP (dBm)
$(x_1^{\text{ref}}, y_1^{\text{ref}})$	1	\mathcal{G}_1	RxLev#1
$(x_2^{\text{ref}}, y_2^{\text{ref}})$	2	\mathcal{G}_2	RxLev#2
	•		
$(x_R^{\text{ref}}, y_R^{\text{ref}})$	R	\mathcal{G}_R	RxLev#R

From above, we have $d(L_{i,j}, L_{i,j+1}) \approx \mathbf{c}_i$ (provided $\mathbf{c}_i \ll \mathbf{r}_i^*$, as we can see in Fig. 7). Hence,

$$\mathbf{b}_i \approx 360 \cdot \mathbf{c}_i / (2\pi \cdot \mathbf{r}_i^*)$$
 degrees. (5)

So, the resulting total number of SZs is $J_i = \lceil 2\pi \cdot \mathbf{r}_i^*/\mathbf{c}_i \rceil$, and hence j should range between 0 and $J_i - 1$. It should now be clear how UA- gNB_i circulates around ref- gNB_i , searching for X-UEs.

To implement the scheme above in practice, $UA-gNB_i$ can use the Discontinuous Transmission (DTX) technique [25] while moving along the path of the cell edge. In doing so, it does not transmit its RF signal while moving from one SZ to another. For example, while moving from position $L_{i,j}$ to $L_{i,j+1}$ (shown in Fig. 7), $UA-gNB_i$ refrains from broadcasting its RF signal. More specifically, RF transmission is necessary only when $UA-gNB_i$ is positioned at location $L_{i,j}$, screening the corresponding SZ; this will save battery power in $UA-gNB_i$ and increase its functional lifetime.

Once the whole screening process is complete, each *UA-gNB_i* generates an information table, as detailed in Table 2. This table will be shared with the corresponding *ref-gNB*; the latter will process the incoming information in conjunction with its own association table (see Table 3) to generate the necessary *UEBCM* and *PDRFC*—that is, each *ref-gNB* will have its own *UEBCM* and *PDRFC*.

10 Time cost for discovery and relocation

Before starting the screening process (Section 6.2), each *UA-gNB* needs to discover a *ref-gNB* for acquiring system information. Once completing this process, the *UA-gNB* relocates to the *ref-gNB* cell edge (according to (3)). These two processes consume time, which we consider below.

10.1 Discovery time cost

We now calculate the time required for a UA-gNB (the ith, say) to discover a ref-gNB. As detailed in Section 6.1.1, UA- gNB_i starts at its initial location, (x_k^{ua}, y_k^{ua}) , according to the CCBS. At this point, UA- gNB_i will need to find and synchronize with ref- gNB_i . To do so, it initiates the CSP, receiving and decoding what is called Cell System Information (CSI) [22]. Two necessary signals, called Primary Synchronization Signal (PSS) and Secondary Synchronization Signal (SSS), must be obtained to get the PCI and frame timing of the detected ref- gNB_i .

The total discovery time, denoted by $T \operatorname{dis}_i$, required for UA- gNB_i to discover ref- gNB_i consists of two parts. The first is the time required to obtain the CSI, which we call T_{csi} . The second is the time required to process the CSI. We introduce a symbol $\eta_i > 0$ such that the second part, the processing time, is $\eta_i T_{csi}$. So η_i is a measure of how fast the CSI can be decoded, normalized by T_{csi} . The higher the processing capability of UA- gNB_i , the smaller the value of η_i . We can now write the following expression:

$$T \operatorname{dis}_{i} = T_{\operatorname{csi}} \cdot (1 + \eta_{i}). \tag{6}$$

The value of T_{csi} is in turn given by

$$T_{\rm csi} = 10 \cdot TTI \cdot SFN, \tag{7}$$

where *TTI* is the *Transmission Time Interval (TTI)* relevant to one subframe, and *SFN* is the *System Frame Number (SFN)*, used to define different system frame cycles [22]. In LTE, a single radio frame comprises 10 subframes; hence the factor of 10 in (7).

10.2 Relocation time cost

As detailed in Section 6.1.2, the location of UA- gNB_i should be at the cell edge of ref- gNB_i . Specifically, the UA- gNB_i should move from its initial location, (x_k^{ua}, y_k^{ua}) , toward the cell edge of ref- gNB_i by a distance equal to $(\mathbf{r}_i^* - \mathbf{r}_i)$, where \mathbf{r}_i^* and \mathbf{r}_i are defined in (1) and (3), respectively $(\mathbf{r}_i \leq \mathbf{r}_i^*)$. From here on, we assume that all the deployed UA-gNBs move in their horizontal plane with equal radial velocity, denoted by v_r . To calculate the required time, denoted by $Trel_i$, for the UA- gNB_i to relocate its initial location (to reach the cell edge), we have the following formula:

$$Trel_i = \frac{\mathbf{r}_i^* - \mathbf{r}_i}{v_r}.$$
 (8)

By (6)–(8), the total time (for discovery and relocating) is

$$T tot_i = 10 \cdot TTI \cdot SFN \cdot (1 + \eta_i) + \frac{\mathbf{r}_i^* - \mathbf{r}_i}{v_r}. \tag{9}$$

It should be clear now that the average time, denoted by T_{ave} , required for the all detected ref- gNB_i (i.e., R) can be written in the following form using (6)–(9):

$$T_{\text{ave}} = T_{\text{csi}} + \frac{T_{\text{csi}}}{R} \sum_{i=1}^{R} \left[\eta_i + \frac{\mathbf{r}_i^* - \mathbf{r}_i}{T_{\text{csi}} \cdot v_r} \right]. \tag{10}$$

As we see from the last formula, many factors can impact the total average time. In the next section, for the purpose of simulation, we assume that R, v_r , and \mathbf{r}_i^* are predefined.

10.3 Simulation setup

To empirically evaluate the required time to discovery and relocating (Tdis $_i$ and Trel $_i$), we use (9) and (10) for the simulation and evaluation. Based on the above assumptions, we set the following parameters: K = 20 (i.e., 20 ref-gNBs in a RoI—K is also the number of the formed clusters, as detailed in Section 6.1.1), $v_r = 1$ m/s, and $\mathbf{r}_i^* = 70$ m. The value of $\mathbf{r}_i^* = 70$ m is typical of small picocells or large femtocells. The speed of 1 m/s for the UAV we set above represents a rather slow-flying vehicle; we use this value to make our experimental scenario very conservative, generating experimental results conservatively (worse than can be expected in practice). More practically realistic values for the speed would result in even better results than we show here.

According to the LTE system specification, we set $TTI = 1 \, msec.$ and SFN = 1024—this is the maximum value that should be assigned to the SFN and refers to the total number of the system frames, which are necessary to acquire all the system information, resulting in $T_{csi} = 10.24 \, sec.$ For η_i and \mathbf{r}_i , we set their values according to uniform distributions in the range of 0.1–0.9 and 10–70 m, respectively.

Fig. 8 illustrates the variation of Ttot $_i$. We can see that the values of Ttot $_i$ lie in the range of 16.45–66.73 sec. This is a reasonable time to act in emergency situations. The average time to complete the two processes is $T_{ave} = 38.06 sec$. Of course, if the deployed UA-gNBs were to have higher speed (v_r) or higher processing capability (lower η_i), the time cost for discovery and relocation would be lower (as quantified in (9)).

11 Generating crisis maps, UEBCMs

After aggregating all the necessary data (as in Table 2) from the associated UA- gNB_i , each ref- gNB_i will generate its own UEBCMs for the area around its cell edge and beyond (including the in-cell area), having information about the surviving UE distributions. That is, the generated UEBCMs should give sufficient awareness to the PSAs such that they

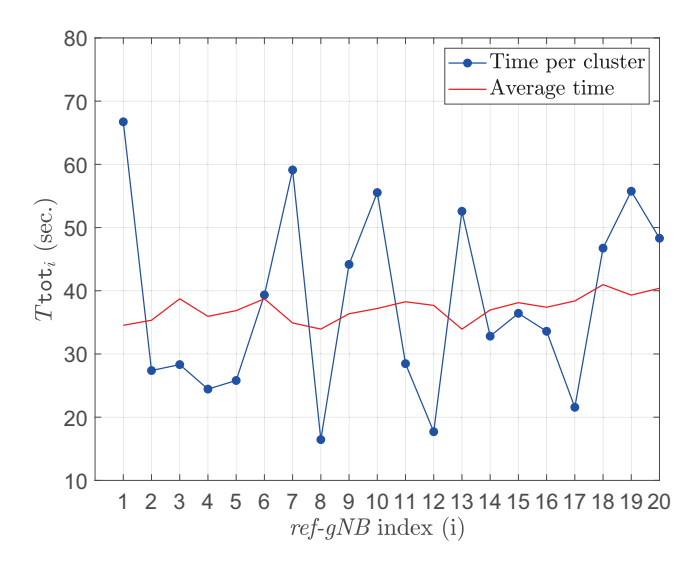


Fig. 8 Discovery and relocation time

have enough knowledge about where the survivors are collected, prioritizing the SAROs in a quick way. For that purpose, we generate two types of *UEBCMs*, which we describe in Sections 11.2 and 11.3, after we introduce an illustrative scenario in the next subsection.

11.1 Illustrative scenario setup

To illustrate how to generate the *UEBCMs*, we consider a simple scenario with one ref- gNB_i and its associated UA- gNB_i (recall the searching procedure of Section 6.1). The same process applies to each ref-gNB in the RoI. To use the searching procedure of Section 6.2, we set the necessary parameters as follows. We set $\mathbf{c}_i = 40 \ m$ and $\mathbf{r}_i^* = 70 \ m$ (cell radius of UA- gNB_i and ref- gNB_i , respectively), resulting in $\mathbf{b}_i = 32.74^\circ$ and $J_i = 11$ (i.e., $\mathcal{L}_i = \{L_{i,j} : j = 0, 1, \dots, 10\}$). The values we set for \mathbf{c}_i and \mathbf{r}_i^* are typical of small picocells or large femtocell [26].

After completing the searching process, we have all the information needed to produce the picture illustrated in Fig. 9, which shows the attached UEs corresponding to each SZ, including the in-cell UEs. In this example, the solid blue circles refer to centers of the SZs, denoted by $R_{i,j}$ —that is, for each $L_{i,j}$, there is a corresponding $R_{i,j} = (\mathbf{r}_i^* + \mathbf{c}_i)/j \cdot \mathbf{b}_i$ (similar to the formula in (4)). The UEs around each $R_{i,j}$ are associated with the corresponding SZ j, z_i^j (i.e., where they are screened and discovered). Each z_i^j has its own UEs as shown in the multi-colored circles in Fig. 9.

To further clarify, we now characterize this illustrative scenario using the detailed notation from Section 5.2. The set of ref-UEs is equal to $G_i = \{ue_{i,1}^{ref}, ue_{i,2}^{ref}, \dots, ue_{i,63}^{ref}\}$. The set of UA-UEs within the $SZ \ j = 0$ is equal to $S_i^0 = \{ue_{i,1}^0, ue_{i,2}^0, \dots, ue_{i,80}^0\}$. Similarly, the set of UA-UEs within

zone j=1 is equal to $S_i^1=\{ue_{i,1}^1,ue_{i,2}^1,\ldots,ue_{i,12}^1\}$, and so on for the others z_i^j . This represents the distribution of UEs in the SZs, which is defined by $Z_i=\{z_i^0,z_i^1,\ldots,z_i^{10}\}$. With the information now gathered, we are ready to produce two types of UEBCMs, as described in the next two subsections: one to show UE densities, and a second one to show UE RSRP levels.

11.2 UEBCM for UE densities

Based on the preceding information, the corresponding refgNB generates a UEBCM for the impacted area, giving visual information about the potential survivor distribution. Specifically, the ref-UEs and UA-UEs in UE-based SAROs have become human sensors for the survivors in the RoI. Accordingly, the ref-gNB will generate a map for the survivor density distribution (shown in Fig. 10). As we can see from this example map, based on the previous illustrative scenario, the majority of individuals are clustered toward the north-west, far from the center of the ref-gNB, which is located at (50, 50). Furthermore, another area with a significant number of individuals is located to the east of the ref-gNB. These two areas contain about 75% of the individuals; these should have higher priority than other regions to be considered for SAROs. The areas with darker colors should be given lower priority, which are located to the far south and north-east (illustrated in dark blue in Fig. 10). This will help the PSAs to act quickly, prioritizing their SAROs to find the majority of the disaster victims.

11.3 UEBCM for UE RSRP levels

Based on the received RSRP levels during the screening procedure, the ref-gNB will generate another useful map, as Fig. 11 illustrates. We can observe from this map that some UEs receive high RSRP levels (approximately -40 to $-70 \, dBm$), especially in the yellowish (and yellowish-green) areas. These levels are (likely) associated with outdoor UEs (located in some particular areas, shown in Fig. 11). Likewise, we can see areas in dark blue in Fig. 11, representing low levels of RSRP. These levels are (likely) received from indoor UEs (experiencing high PL); they might be stranded inside buildings and need immediate help. This gives rise to a significant observation, as we illustrate in the following. As detailed in Fig. 10, one area that has the majority of individuals is located toward the north-west. When comparing this specific area with the corresponding RSRP levels map (Fig. 11), we notice that these UEs are likely to be indoors. Specifically, we can conclude that this particular area is high-density cluster of UEs that are experiencing high PL. This area would thus be given high priority for SAROs rela-

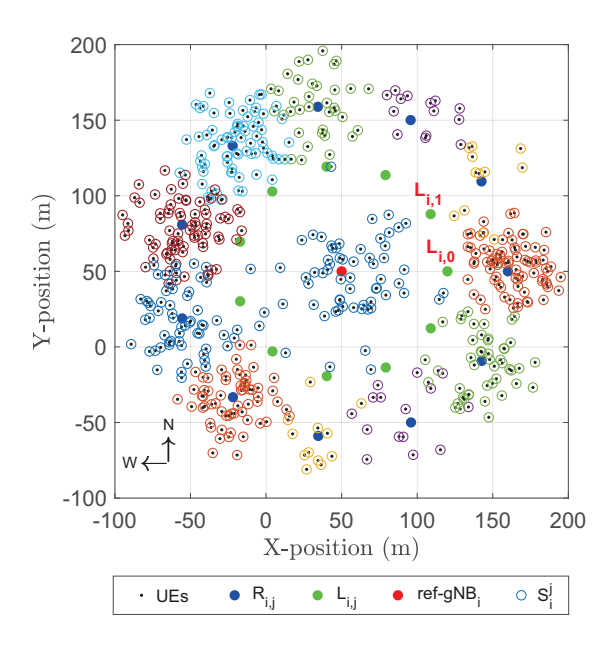


Fig. 9 Attached UEs corresponding to each SZ

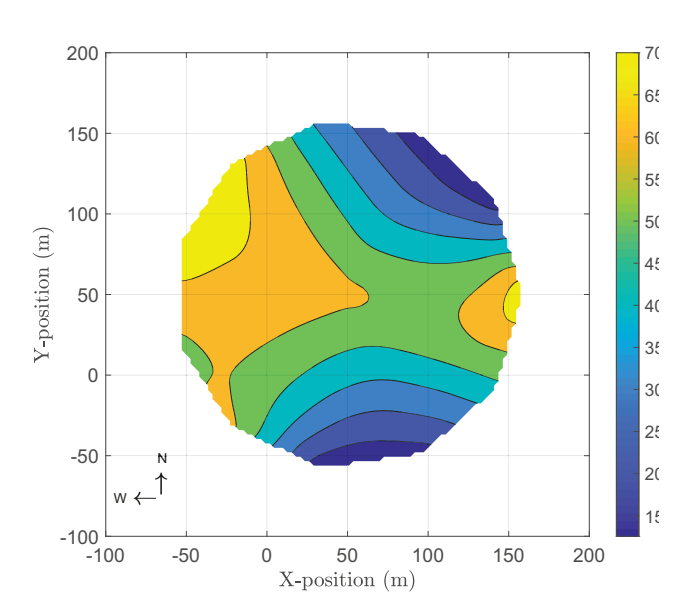


Fig. 10 UEBCM: Density of surviving UEs

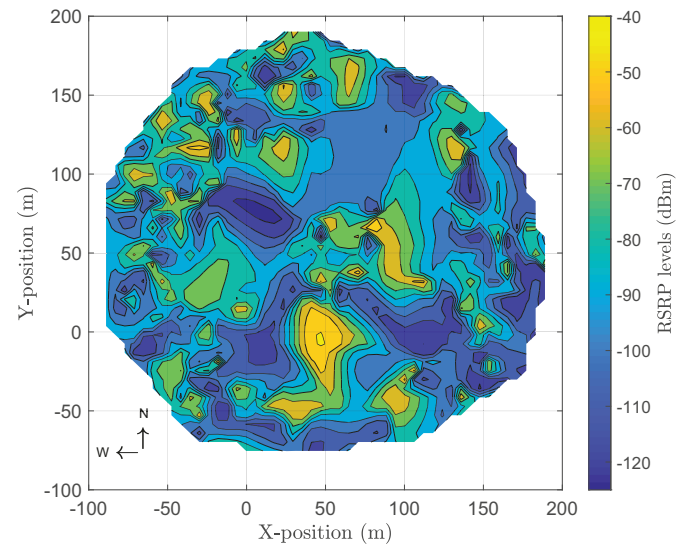


Fig. 11 UEBCM: RSRP levels of the attached UEs

tive to other areas. Based on this, we can generate a *PDRFC*, as described next.

11.4 Building Priority-Driven RFC (PDRFC)

As defined in Section 5.1, the *PDRFC* is used to identify areas that need immediate RFC. Based on the extracted information from the preceding maps (Sections 11.2 and 11.3), Table 4 is built, providing priorities on where immediate RFC is needed (based on UE clustering). Clearly, z_i^0 , z_i^5 , z_i^4 , and z_i^7 need immediate RFCs; the majority of survivors

Table 4 Information table for the *PDRFC*

SZ index	Priority index	UA-gNB locations (polar)	UE densities
z_i^0	0	$L_{i,0}$	80
z_i^5	1	$L_{i,5}$	77
z_i^4	2	$L_{i,4}$	75
z_i^7	3	$L_{i,7}$	62
z_i^1	10	$L_{i,1}$	12

can be found there. This can be achieved by deploying dedicated *UA-gNBs* hovering over these zones, providing semi-permanent RFC.

In summary, the vital information provided by *UEBCMs* and *PDRFC* enables the PSAs to provide SAROs for the largest number of survivors in a prioritized way.

12 Conclusion

In this paper, we have described a new framework for SAROs (called *UE-based SAROs*) post-disaster to find and locate survivors based on the idea that most individuals have their own UEs—potentially, they are still alive and need to be rescued. Our framework, *UE-based SAROs*, addresses the following concerns. 1) With the lack of RFC, how do we give the corresponding PSAs better awareness on the individual locations in the RoI without their assistance (for life-saving purposes)? 2) What is the quickest way to recover the RFC right after disasters, exploiting the surviving gNBs (i.e., *ref-gNBs*), before it becomes too late, especially considering that most UEs are battery limited? 3) Based on the fact that finding and locating survivors is more important than providing RFC elsewhere, where are the majority of survivors located and how (indoor or outdoor)?

UE-based SAROs provide vital information to the PSAs to prioritize their operations and manage the available resources. By considering the surviving UEs as human-based sensors distributed in the RoI and are able to exchange signaling messages without active user participation, the UE-based SARO provides the following benefits: 1) right after disasters, it generates immediate visual crisis maps, UECBMs, showing the potential survivor distribution, 2) it provides quick vital information about which regions contain the majority of survivors, and 3) based on the preceding information, the PSAs can prioritize and manage their SAROs effectively, providing the necessary RFC accordingly.

Finally, *UE-based SAROs* provide PSAs with situational awareness about the disaster-impacted area quickly and even before they arrive at the scene, keeping the PSAs better informed about locations of the disaster victims. This enables the PSAs to serve the largest number of survivors in a timely manner even when the cellular communication infrastructure is partially dysfunctional.

Acknowledgements The first author was supported by the Iraqi Ministry of Higher Education and Scientific Research through scholarship under Grant 4650/11/16/2014. This work was supported in part by the National Science Foundation under grant CMMI-1638284.

References

 3GPP TR 22.862 v14.1.0: Feasibility study on new services and markets technology enablers for critical communications; stage 1 (release 14) (2016). http://www.3gpp.org

- 3GPP TS 22.179 v16.4.0: Mission Critical Push To Talk (MCPTT); stage 1 (release 16) (2018). http://www.3gpp.org
- 3. 3GPP TS 23.401 v14.4.0: General Packet Radio Service (GPRS) enhancements for Evolved Universal Terrestrial Radio Access Network (E-UTRAN) access (release 14) (2017). http://www.3gpp.org
- 3GPP TS 23.468 v15.0.0: Group Communication System Enablers for LTE (GCSE_LTE); stage 2 (release 15) (2018). https://www.etsi.org
- 3GPP TS 24.334 v15.2.0: Proximity-services (ProSe) User Equipment (UE) to ProSe function protocol aspects; Stage 3 (release 15) (2018). http://www.3gpp.org
- 3GPP TS 36.133 v14.5.0: Requirements for support of radio resource management (2017). http://www.etsi.org/standards-search
- 7. 3GPP TS 36.213 v15.2.0: Physical layer procedures (release 15) (2018). http://www.3gpp.org
- 8. 3GPP TS 36.214 v14.4.0: Physical layer; Measurements (release 14) (2018). http://www.3gpp.org
- 9. 3GPP TS 36.304 v14.3.0: User Equipment (UE) procedures in idle mode (release 8) (2017). http://www.3gpp.org
- 3GPP TS 36.331 v14.3.0: Radio Resource Control (RRC); Protocol specification (release 14) (2017). http://www.3gpp.org
- 11. 3GPP TS 36.422 v15.0.0: X2 signaling transport (release 15) (2018). http://www.3gpp.org
- 12. 3GPP TS 36.942 v15.0.0: Radio Frequency (RF) system scenarios (release 15) (2018). http://www.3gpp.org
- 3GPP TS 38.300 v15.0.0: NR; NR and NG-RAN overall description; Stage 2 (release 15) (2017). http://www.3gpp.org
- Abusitta, M.M., Dama, Y., Abd-Alhameed, R.A., See, C.H., Noras, J., Adebola, A., Excell, P.: Beam steering of horizontally polarized circular antenna arrays. In: 2011 Loughbrgh. Antennas Propag. Conf., pp. 1–4. IEEE (2011). DOI 10.1109/LAPC.2011.6114126
- Ali, K., Nguyen, H.X., Shah, P., Vien, Q.T., Bhuvanasundaram,
 N.: Architecture for public safety network using D2D communication. In: 2016 IEEE Wirel. Commun. Netw. Conf. Work., pp. 206–211. IEEE (2016). DOI 10.1109/WCNCW.2016.7552700
- Ali, K., Nguyen, H.X., Vien, Q.T., Shah, P., Chu, Z.: Disaster management using D2D communication with power transfer and clustering techniques. IEEE Access 6, 14643–14654 (2018). DOI 10.1109/ACCESS.2018.2793532
- Alsaeedy, A.A.R., Chong, E.K.P.: Mobility management for 5G IoT devices: Improving power consumption with lightweight signaling overhead. IEEE Internet Things J. (2019). DOI 10.1109/JIOT.2019.2920628
- Alsaeedy, A.A.R., Chong, E.K.P.: Tracking area update and paging in 5G networks: A survey of problems and solutions. Mob. Networks Appl. 24(2), 578–595 (2019). DOI 10.1007/s11036-018-1160-6
- Arthur, D., Arthur, D., Vassilvitskii, S.: K-means++: the advantages of careful seeding. Proc. 18TH Annu. ACM-SIAM Symp. Discret. ALGORITHMS (2007). http://citeseerx.ist.psu.edu/viewdoc/summary?doi=10.1.1.360.7427
- Asadi, A., Wang, Q., Mancuso, V.: A survey on device-to-device communication in cellular networks. IEEE Commun. Surv. Tutorials 16(4), 1801–1819 (2014). DOI 10.1109/COMST.2014.2319555
- 21. AT&T Newsroom: All 50 U.S. States, 2 Territories and the District of Columbia Opt-In to FirstNet (2017). http://www.5gamericas.org/en/newsroom/member-news/all-50-us-states-2-territories-and-district-columbia-opt-firstnet/
- 22. Dahlman, E., Parkvall, S., Skold, J.: 4G, LTE-advanced pro and the road to 5G, 3rd edn. Academic Press (2016)
- Deruyck, M., Wyckmans, J., Joseph, W., Martens, L.: Designing UAV-aided emergency networks for large-scale disaster scenarios. EURASIP J. Wirel. Commun. Netw. 2018(1), 79 (2018). DOI 10.1186/s13638-018-1091-8. https://doi.org/10.1186/s13638-018-1091-8

- Fodor, G., Parkvall, S., Sorrentino, S., Wallentin, P., Lu, Q., Brahmi, N.: Device-to-Device communications for national security and public safety. IEEE Access 2, 1510–1520 (2014). DOI 10.1109/ACCESS.2014.2379938
- Frenger, P., Moberg, P., Malmodin, J., Jading, Y., Godor, I.: Reducing Energy Consumption in LTE with Cell DTX. In: 2011 IEEE 73rd Veh. Technol. Conf. (VTC Spring), pp. 1–5. IEEE (2011). DOI 10.1109/VETECS.2011.5956235
- Fujitsu Network Communications Inc.: High-capacity indoor wireless solutions: Picocell or Femtocell? Tech. rep. (2013). https://www.fujitsu.com/us/Images/High-Capacity-Indoor-Wireless.pdf
- 27. Google.org: https://google.org/crisismap/weather_and_events. https://google.org/crisismap/weather_and_events
- Heisler, Y.: A huge 4G milestone: LTE is now available for 98% of Americans. Tech. rep. (2015). http://bgr.com/2015/03/23/lte-coverage-map-united-states/
- Kaleem, Z., Qadri, N.N., Duong, T.Q., Karagiannidis, G.K.: Energy-efficient device discovery in D2D cellular networks for public safety scenario. IEEE Syst. J. 13(3), 2716–2719 (2019). DOI 10.1109/JSYST.2019.2899922
- Lin, X., Yajnanarayana, V., Muruganathan, S.D., Gao, S., Asplund, H., Maattanen, H.L., Bergstrom, M., Euler, S., Wang, Y.P.E.: The sky is not the limit: LTE for unmanned aerial vehicles. IEEE Commun. Mag. 56(4), 204–210 (2018). DOI 10.1109/MCOM.2018.1700643
- Lorincz, K., Malan, D., Fulford-Jones, T., Nawoj, A., Clavel, A., Shnayder, V., Mainland, G., Welsh, M., Moulton, S.: Sensor networks for emergency response: Challenges and opportunities. IEEE Pervasive Comput. 3(4), 16–23 (2004). DOI 10.1109/MPRV.2004.18
- Masaracchia, A., Nguyen, L.D., Duong, T.Q., Nguyen, M.N.: An energy-efficient clustering and routing framework for disaster relief network. IEEE Access 7, 56520–56532 (2019). DOI 10.1109/ACCESS.2019.2913909
- Mcgrath, S.P., Grigg, E., Wendelken, S., Blike, G., De Rosa, M., Fiske, A., Gray, R.: ARTEMIS: A vision for remote triage and emergency management information integration (2003). http://citeseerx.ist.psu.edu/viewdoc/summary?doi=10.1.1.128.4959
- Merwaday, A., Guvenc, I.: UAV assisted heterogeneous networks for public safety communications. In: 2015 IEEE Wirel. Commun. Netw. Conf. Work., pp. 329–334. IEEE (2015). DOI 10.1109/WCNCW.2015.7122576
- Müller, W., Marques, H., Rodriguez, J., Bouwers, B.: Next-generation infrastructure for public protection and disaster relief organizations.
 SPIE Newsroom (2016). DOI 10.1117/2.1201607.006523. http://www.spie.org/x119789.xml
- Muruganathan, S.D., Lin, X., Maattanen, H.L., Zou, Z., Hapsari, W.A., Yasukawa, S.: An overview of 3GPP release-15 study on enhanced LTE support for connected drones (2018). http://arxiv.org/abs/1805.00826
- Nokia: LTE networks for public safety services (2015). http://networks.nokia.com
- 38. Public Safety and Homeland Security: 2017 Atlantic hurricane season impact on communications. Tech. rep. (2018). https://docs.fcc.gov/public/attachments/DOC-353805A1.pdf
- Ringqvist, P.: The promise of 5G for public safety (2018). https://www.emsworld.com/commentary/1221807/promise-5g-public-safety
- 40. Rowe, M.: Beam steering: One of 5G's components (2018). https://www.edn.com/electronics-blogs/5g-waves/4460861/Beam-steering—One-of-5G-s-components
- Safecom, O.: Land Mobile Radio (LMR) 101 part 1: Educating decision-makers on LMR technologies. Tech. rep. (2016). https://www.dhs.gov/sites/default/files/publications/LMR 101_508FINAL.pdf

- Shakoor, S., Kaleem, Z., Baig, M.I., Chughtai, O., Duong, T.Q., Nguyen., L.D.: Role of UAVs in public safety communications: Energy efficiency perspective. IEEE Access (2019). DOI 10.1109/ACCESS.2019.2942206
- Sharma, S., Pandey, H.M.: Genetic algorithm, particle swarm optimization and harmony search: A quick comparison. In: 2016 6th
 Int. Conf. Cloud Syst. Big Data Eng., pp. 40–44. IEEE (2016).
 DOI 10.1109/CONFLUENCE.2016.7508044
- 44. Singh, A., Kumar, A., Ranjan, A., Kumar, A., Kumar, A.: Beam steering in antenna. In: 2017 Int. Conf. Innov. Information, Embed. Commun. Syst., pp. 1–4. IEEE (2017). DOI 10.1109/ICIIECS.2017.8275895
- Tanner, J.C.: Nokia unveils LTE backpack for critical comms with bonus data aggregation (2017). https://disruptive.asia/nokia-ltebackpack-critical-communications/
- Williams, D.: Tactical medical coordination system (TacMedCS). Tech. rep., NAVAL HEALTH RESEARCH CENTER SAN DIEGO CA (2007). https://apps.dtic.mil/docs/citations/ADA477535
- Zarri, M.: Network 2020: Mission critical communications. Tech. rep., GSMA (2017). www.gsma.com/network2020